IEEE Access
Multidisciplinary | Rapid Review | Open Access Journal

Received September 10, 2018, accepted October 8, 2018, date of publication October 26, 2018,
date of current version November 19, 2018.

Digital Object Identifier 10.1109/ACCESS.2018.2876882

Robustness of Reflection Symmetry Detection Methods on Visual Stresses in Human Perception Perspective

IBRAGIM R. ATADJANOV AND SEUNGKYU LEE
Department of Computer Science and Engineering, Kyung Hee University, Yongin 17104, South Korea

Corresponding author: Seungkyu Lee (seungkyu@khu.ac.kr)

This work was supported by the Ministry of Science and ICT, South Korea, through the Information Technology Research Center Support Program supervised by the Institute for Information and communications Technology Promotion under Grant IITP-2018-2013-1-00717.

ABSTRACT Symmetry is one of the most frequently observed fundamental regularities in the visual characteristic of real-world objects. The human brain has been trained to respond quickly to symmetry patterns, organizing them as salient clues for the unique description of objects. Recently, automatic symmetry detection methods have been widely introduced in computer vision and graphics fields for 2-D and 3-D object data, including reflection, translation, and rotation symmetry patterns. Researchers have invented features inspired by a human vision system and have adopted deep learning approaches. On the other side, traditional performance evaluations have been conducted on a unified test data set containing random degrees of diverse visual challenges. However, they ignore observing the insight of usability and practicality of the methods in higher level tasks, such as object recognition. In this paper, we carefully organize the visual stress data set for reflection symmetry detection evaluation proposing a novel evaluation framework. The state-of-the-art reflection symmetry detection methods are re-evaluated and analyzed in human perception perspective.

INDEX TERMS Reflection symmetry, performance evaluation, human symmetry perception, visual stresses, psychophysics.

I. INTRODUCTION

Symmetry is ubiquitously observed phenomena in both natural [1] and human-made objects [2], [3]. Many living organisms such as birds [4], animals [5] and insects [6]–[8] perceive symmetry patterns of the natural environment. It has been studied that there exists a significant correlation between symmetry and aesthetics, excellence in manufacturing and health [4], [5], [9]–[11]. Symmetry perception is also the matter of survival for jungle animals helping them recognize the natural enemy. Because symmetry is fundamentally inherent to objects of this world, symmetry perception is evolved as a crucial necessity for visual object recognition for humans as well [12]. It is determined that human can perform core object recognition task in a fraction of seconds [13]. The human object recognition process, which is believed to be performed in the ventral visual stream of the brain cortex, consists of multiple stages: line and edge detection [14]–[17], shape representation (e.g. grouping the stimuli coming from retina's visual sensors) [18]–[21] and symmetry perception [22], [23]. Being in complex interaction with object recognition in the human brain, symmetry perception is a preattentive process.

Due to the critical role of symmetry patterns in perceiving and understanding our world, automatic symmetry detection has been widespread interest in many research fields such as neuroscience [24], psychology, and computer science [2]. For the last few decades, researchers introduced numerous computational symmetry detection methods [25], [26]. However, symmetry detection from real-world images is still a challenging task in computer vision and pattern recognition. There have been several symmetry detection competitions [26]–[28] on public evaluation dataset for diverse symmetry types. Our observation on such evaluations of symmetry detection methods is that traditional evaluation scheme calculates a score and ranking based on a single fixed public dataset, but it does not provide detailed insight into strength and weakness of each method for its further improvement. Even though their dataset contains real-world images of diverse visual challenges, single performance score on entire images of the dataset does not demonstrate different

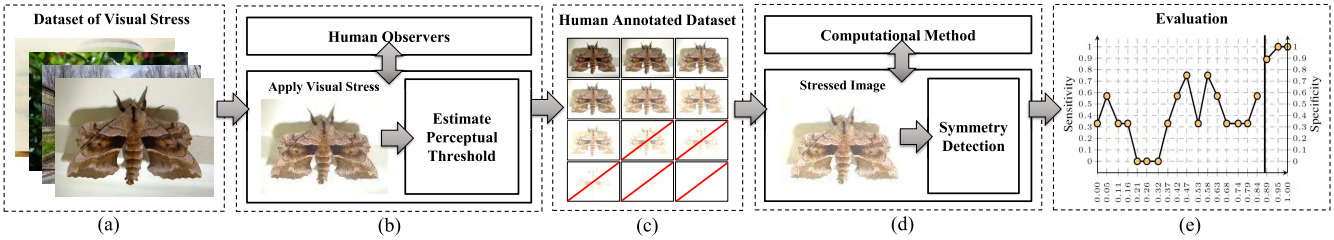

FIGURE 1. The workflow of the proposed work. (a) Provided images for each visual stress type, (b) determine the human perception threshold for each visual stress type and (c) generate a human organized dataset for each stress type. (d) Evaluate computational symmetry detection methods on the human organized dataset and demonstrate behavior and robustness of computational methods on each visual stress type.

behaviors of methods on those visual challenges. If the reaction of a detection method for each challenging point could be evaluated individually, we could leverage the improvement of the method rather than just evaluating it. Recently in [29], Nagar and Raman propose a reflection symmetry map and measures the performance of symmetry detection based on the detected correspondences rate. In [30], Nagar and Raman evaluate the robustness of their reflection symmetry detection method against various distortions in the 3D point cloud. However, these evaluation techniques are not suitable for 2D reflection symmetry detection methods on real-world images. It is not a trivial task to accurately label symmetry correspondences for each pixel in a 2D image. Furthermore, it is not possible to perturb locations of pixels in a 2D image as they demonstrated with a 3D point could [30].

In this work, we propose a novel evaluation framework for computational reflection symmetry detection methods in human perception perspective. Unlike traditional evaluation techniques, the proposed framework demonstrates the performance behavior of reflection symmetry detection methods on the visual stress dataset that is carefully organized based on the investigation of human perception. Stressed image samples are categorized into symmetry or non-symmetry groups based on human evaluator study. For accurate categorization, we psychophysically determine the absolute threshold of human symmetry perception on each visual stress by conducting an experiment with 25 human evaluators. The threshold values are determined for each of the 11 visual stress types which are under consideration in this work. In order to comparatively verify the validness of the thresholds for each stress type, we conduct an additional psychophysical experiment to discover the thresholds for each image of those degradation types. The workflow of the proposed work is illustrated in Fig. 1. Followings summarize contributions of the proposed work:

- A new evaluation dataset for reflection symmetry detection consists of eleven visual stress types with careful annotation based on human perception: We build a web-based interface to collect psychophysical decision level of human symmetry perception for the eleven visual stresses.
- A novel evaluation framework for computational reflection symmetry detection methods in human perception perspective over the visual stresses.
- An analytic evaluation with three state-of-the-art reflection symmetry detection methods using the proposed evaluation framework.

II. BACKGROUND AND RELATED WORK

The proposed evaluation framework for computational reflection symmetry detection methods is built upon the knowledge in two emerging directions of symmetry study: (1) human symmetry perception, and (2) computational symmetry detection methods.

A. HUMAN SYMMETRY PERCEPTION

The origin of human symmetry perception studies dates far back to XIX century [31]. Since then, the numerous concepts of modeling human symmetry perception process are proposed and empirically validated by conducting various psychophysical experiments [3]. In order to understand internal brain processes responsible for symmetry perception, researchers of neuroscience [32] and psychophysics [23] fields investigated human brain activities using fMRI (Functional Magnetic Resonance Imaging). They observed a correlation between symmetry perception and activations in V3A, V4, V7 and LO, DLO regions of brain cortex [22], [33]. Regarding work of Tyler [34], the symmetry detection is three stages of processes: (1) elaboration of dimensionality of stimuli properties and passing the information to neural analyzers that impose varieties of symmetries; (2) the self-matching feed-forward process that is performed in parallel on each feature across all possible symmetries; (3) the active and manipulative recognition process, which identifies object properties that are too complex to perform at previous stages. Despite extensive experiments and researches dedicated to understanding the mechanics and physics of human symmetry perception, it is still unclear how the human brain perceives symmetry such effortlessly, and what exact neural processes are responsible for it.

Among symmetries, reflection symmetry is more salient type [35] for humans. Researchers vastly studied reflection symmetry and psychophysically revealed the properties that attract human perception [35]–[50]. Regions supporting the symmetry structure are called the integration regions. The perturbations and distortions in those integration regions are perceived much easily [35]–[38] by humans. The shape and size of the integration region of reflection symmetry

pattern scale along with its spatial frequencies [39]. Authors psychophysically determined that the integration region is 2:1 aspect ratio radii ellipse where longer radius equals the length of the reflection line. As eccentricity increase in human eye retina, the integration region of symmetry gets narrower [40]. In other words, the symmetry pattern that falls on the peripheral vision has a narrow integration region. Therefore, symmetry detection is found preattentive only in fovea area of the retina [41]. However, it is still possible to discriminate and detect symmetry in the periphery area of the retina, but that symmetry pattern has small perceptual strength [38], [42]. The orientation of the symmetry pattern has a little effect on symmetry detection [43], [44]. However, the orientations of supporting features in the integration region of the symmetry pattern have a considerable impact to the robustness of symmetry perception; humans have the higher robustness to features orthogonally oriented to symmetry axis than to those that have parallelly oriented [45]. Human symmetry perception is robust to distortions caused by perspective projection too. Moreover, the perception of skewed symmetries helps to perceive the orientation of 3D surfaces which contain those skewed symmetries [46]. Therefore, the perception of skewed symmetries is a crucial tool in the judgment of object orientations in space [47]. Another interesting outcome of psychophysical experiments shows that having the opposite contrast on reflected feature pairs makes the symmetry pattern imperceptible [48]–[50].

In order to adopt the properties of human symmetry perception into computational symmetry detection methods, researchers introduced a goodness measure for symmetry patterns. Symmetries with high goodness are detected easily by a human. Van der Helm and Leeuwenberg [51], [52] introduced a holographic model which measures the goodness of symmetry pattern as a ratio between the number of features supporting the symmetry and the number of all features. The model does not care about the qualitative properties of features and quantitatively measures the goodness. Wagemans proposed a qualitative model - the bootstrap model - which exploits the features' orientations and locations in the visual field, perturbation information, and groupings as summarized in [53]. Later, with the initiative of Wagemans *et al.* [54], van der Helm and Leeuwenberg [55], [56] and Nucci and Wagemans [57] showed how his quantitative goodness model could be combined with qualitative bootstrap model. Dakin and his colleagues also introduced qualitative (process) models that consider eye fixation information, the orientation of the features, size and shape of the integration region [39], [41], [58].

B. COMPUTATIONAL SYMMETRY DETECTION METHODS AND EVALUATION

Reflection symmetry is one of the most occurred regularities, and it has considerable insight into object recognition and scene understanding. Many researchers were devoted to finding practical and robust computational reflection symmetry detection solutions for a few decades as summarized in [2]. A decade ago, the authors pointed out challenges that are needed to be addressed in order to utilize the favor of symmetry for artificial intelligence. Since then, various approaches were proposed and evaluated in competition workshops of high-level conferences like [26]–[28]. Lately, shape and structure information of an object gained more interest for symmetry detection. Methods utilizing this information for symmetry detection have shown improvements in challenging natural images [59]–[61]. Latest appearance (color, texture) [61], [62] and patch-kernel based methods [63]–[65] also, achieved the state-of-the-art performance by exploiting symmetry detection task as energy minimization [62], registration [66] and linear assignment problem [30]. Despite the interest in, and the number of works on symmetry detection has been increasing year by year, the state-of-the-art method of last decade still competitive with current ones. Based on last symmetry detection competition workshop [26], the method proposed in [67] even outperformed the current state-of-the-art on multiple symmetries detection in 2D real-world dataset.

The evaluation method proposed in symmetry detection competition workshop [27] is accepted and being used as a standard evaluation for most of the computational symmetry detection papers proposed since. As mentioned by researcher multiple times, the analytical evaluation of the symmetry is a nontrivial task. The rules for determining the correct detection is decided empirically and not always achieved a fair evaluation. In [60], Atadjanov and Lee demonstrated one of the weak sides of the traditional evaluation method which evaluates the performance having a limited amount of ground truth information. They demonstrated that the ground truth set for multiple symmetries datasets does not include all potential symmetries. Considering the detection of provided ground truth symmetries as true positives is not a fair evaluation for a method that can detect other unlabeled potential symmetries. Therefore, the authors additionally evaluated the performance by judging each detected axis by human evaluators.

We have encountered different kinds of method evaluations in the recent state-of-the-art symmetry works. Nagar and Raman [29] provided the evaluation that shows the behavior of their symmetry map generation method. They evaluated reflection correspondence rate based on the distance measure between estimated reflection correspondence points and ground truth correspondence. They showed that their method achieves more improved symmetry map as the number of iterations increase in their method. By this, they proved the convergence of the proposed iteration based method. The evaluation they provide shows the behavior of their method over increasing iterations which does not match with our purpose and that evaluation is only specific to their proposed method algorithm, which is iteration based. In [30], Nagar and Raman provide reflection symmetry plane detection for 3D cloud points. In order to show the robustness of their detection method for visual distortions, they evaluate their method by applying perturbations to the cloud

data with different perturbation variances. To our point of view, this method is useful to show the performance as a behavioral function of perturbations. However, the method is not mature and need to be generalized in order to be applied universally for all possible symmetry works. For example, they applied the perturbation to the 3D point cloud, which is not possible for 2D real-world images. Our proposed framework demonstrates behavior for more broader, specific visual stresses which more likely covers real-world scenarios and uses human symmetry perception as a reference.

C. SIMILAR WORKS IN OTHER FIELDS

Recently, researchers of object recognition field proposed a comparative evaluation of deep neural networks against humans on images under various visual stresses [68], [69]. In [68], Geirhos *et al.* use four visual stress types: color, contrast, noise, and eidolon. For the color experiment, the authors compare detection rates on two, color and grayscale, conditions. For each noise and contrast stress type, the authors use fixed eight stress levels. In eidolon-experiment, 24 different conditions were employed. In [69], Dodge and Karam utilized blur and noise visual stress type, with only five different stress levels (standard deviation). In the experiment, participants are asked to categorize the presenting image into a fixed number of categories. All work showed that as the intensity of stress increase, human detection achieves better performance than computational methods. To our knowledge, the experimental method that is utilized in [69] is inadequate. The method presents images with descending stress level and stops at the stress level where a participant successfully recognizes the stressed image. So, an accidental miss-response from a participant makes the result of the experiment invalid. Nevertheless, in both works above, the intensities of the visual stress seem to be sampled by the power law (or Weber-Fechner law). However, we doubt that human symmetry perception and visual stress intensity follows Weber-Fechner law. For example, in [70], van der Helm reported that detection of symmetry in the presence of noise does not follow Weber-Fechner law, but it follows the psychophysical law that holds for glass pattern. Moreover, our proposed work utilizes multiple other visual stress types, and we cannot know the underlined relationship between the human symmetry perception and each of those visual stress types. Therefore, we adopt the up-down staircase method [71] with variable step-size in order to determine the absolute threshold of each visual stress type carefully. The threshold indicates human symmetry perception limit. Please, refer to the literature [72] for detailed information about psychophysics and psychophysical methods.

III. VISUAL STRESS DATASET IN HUMAN SYMMETRY PERCEPTION PERSPECTIVE

Human symmetry perception is robust to various visual stresses. We define 11 visual stress types on reflection symmetry patterns. We psychophysically find the absolute threshold for each visual stress type. The absolute threshold is the biggest intensity level of visual stress (the smallest intensity level of stimulus) at which a human still can perceive the symmetry. Next, we conduct two psychophysical experiments. The first experiment determines the absolute threshold for each image of all visual stress types. The second experiment determines the absolute threshold for each visual stress type.

A. VISUAL STRESS TYPES

In this work, we define five primitive types of visual stresses: (1) blurring, (2) brightness, (3) additive white noise, (4) size/resolution, and (5) affine skewness. For utilizing the psychophysical method, the relationship between visual stress type and human symmetry perception (sensation) strength should be monotonic; the more significant the amount of visual stress in an image, the less the human symmetry perception strength. This requirement applies to all types of visual stresses except brightness, because, when an image is at perceptually optimal brightness, both the increase and the decrease of brightness cause visual stress. Therefore we divide brightness stress into two types: positive brightness change (brightening) and negative brightness change (darkening). We apply blurring, brightening, darkening and additive white noise in two ways: stress in whole image and stress in one half of reflection symmetry pattern. Stress in one half simulates reflection symmetry pattern on a mirror-like surface such as water surface. Followings are eleven visual stress types evaluated in this work:

- *Blur Half (BH).* Gaussian blurring one half of symmetry pattern in an image. The standard deviation of Gaussian blurring is used to change the strength of visual stress.
- *Blur Whole (BW).* Gaussian blurring the whole image. The standard deviation is used to change the intensity of visual stress.
- *Brightness Half (LH).* Increasing the brightness in one half of symmetry pattern in an image. The intensity of image colors defines the intensity of visual strength.
- *Brightness Whole (LW).* Increasing the brightness of the whole image. The intensity of image colors define the intensity of visual strength
- *Darkness Half (DH).* Darkening one half of symmetry patter in an image. A decrease in the intensity of image color increases the intensity of visual stress.
- *Darkness Whole (DW).* Darkening whole image. A decrease in the intensity of image color increases the intensity of visual stress.
- *Noise Half (NH).* Adding white noise to one half of symmetry pattern in an image. The standard deviation of white noise is used to change the intensity of visual stress.
- *Noise Whole (NW).* Adding white noise to the whole image. The standard deviation of white noise is used to change the intensity of visual stress.
- *Size/Resolution (R).* Changing the size/resolution of an image by a factor. The factor parameter (0 and 1) indicating the change in size is used to change the intensity of visual stress. E.g., 0 means that no change in the

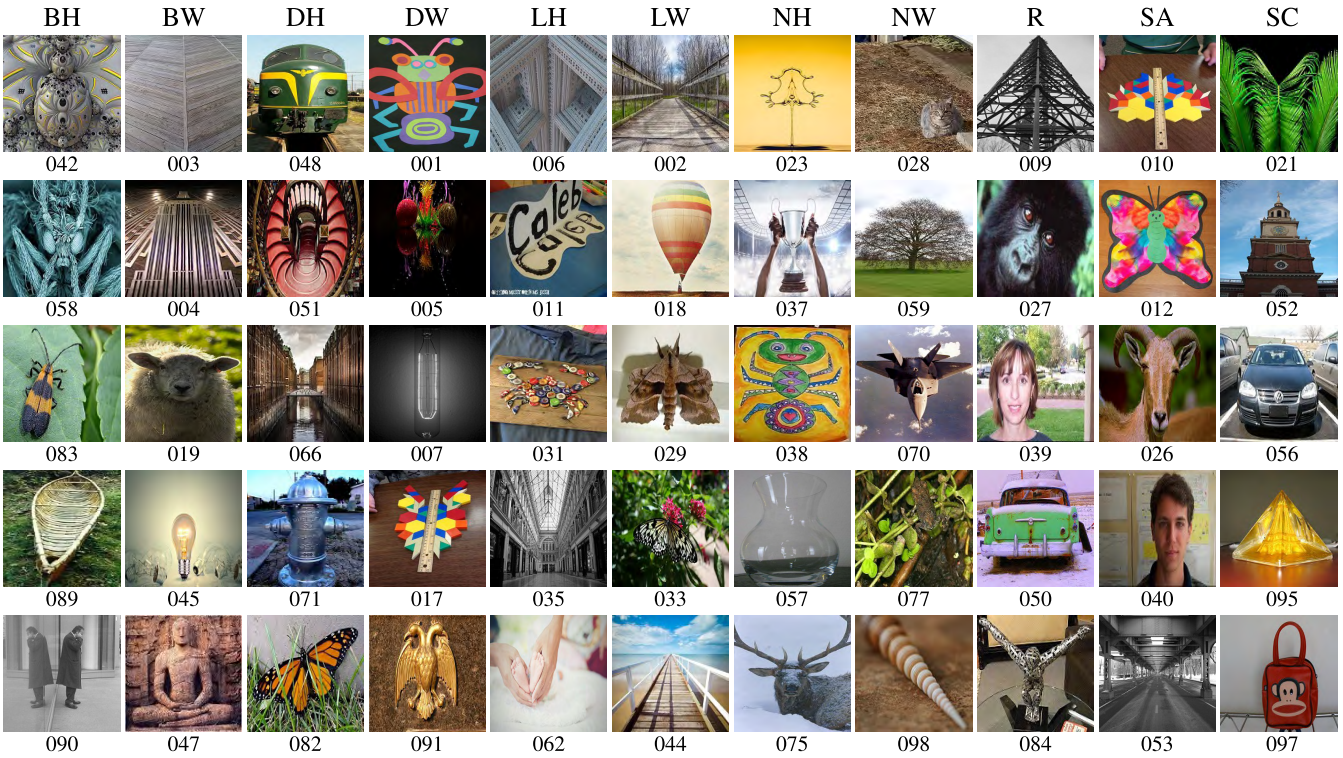

FIGURE 2. Dataset of images for all 11 visual stress type. Columns represent visual stress types and labeled with visual stress labels. Images are taken from ICCV 2017 symmetry workshop [26].

size, 0.5 means that the size is halved, 1 means that the size is 0.

- *Skew Across Symmetry Line (SC).* 3D rotating the image plane across the reflection symmetry axis. The rotation angle is used to change the intensity of visual stress.
- *Skew Along Symmetry Line (SA).* 3D rotating the image plane along the reflection symmetry axis. The rotation angle is used to change the intensity of visual stress.

Fig. 2 presents dataset images for all 11 visual stress types.

B. PSYCHOPHYSICAL METHOD

A visually stressed symmetry image is presented to a participant with the symmetry axis drawn on it. A participant is asked if the image contains a reflection symmetry pattern by provided symmetry axis. The symmetry axis drawn on the image gets the participant's eye fixated on the reflection symmetry pattern of interest. In this work, we are not interested in reaction time or detection time to the symmetry pattern. Therefore, there is no limitation for both stimulus presentation and the participant's response time.

As a psychophysical method, up-down staircases [73] with variable step-size is used. Starting intensity I_s is selected randomly using the following formula.

$$I_s = (b_1 + (b_2 - b_1) * rand()) * I_{max},$$

where I_{max} is upper bound of the visual stress intensity and $0 \leq b_1 < b_2 \leq 1$. Note that lower bound of visual stress intensity is zero. $rand()$ is a function that generates random real number between 0 and 1. Step-size $\triangle I$ is updated when three consecutive reversals occur. The following is the update rule formulation.

$$\triangle I = (l_1 + (l_2 - l_1) * rand()) * \triangle I,$$

where $0 \leq l_1 < l_2 \leq 1$ and defines the constraints of the step-size for the update formulation. Above formulation updates the step-size by a random factor between l_1 and l_2. For each threshold detection procedure, two interleaved staircases are used (see Fig. 3). The first starts with high stress intensity $I_{s1} = (b_1 + (1 - b_1) * rand()) * I_{max}$; second starts with low stress intensity $I_{s2} = (b_2 - 0) * rand() * I_{max}$. In order to decrease the probability of participants guessing the presenting trials content and structure, the visual stress type, the image of that stress type and one of two staircase processes of that image are randomly selected and presented to the participant.

C. WEB BASED UI AND EXPERIMENTAL SETUP

We built a web-based system (tool) in order to conduct the psychophysical experiment for multiple participants simultaneously. Participants are requested to register and attend the experiment. Before the experiment starts, the system provides the participants with the definition of the reflection symmetry with multiple example pictures. Participants are also provided the instruction about the experiment and the user interface. Next, the web-based system provides multiple samples of stressed images for each visual stress type. It is done to help

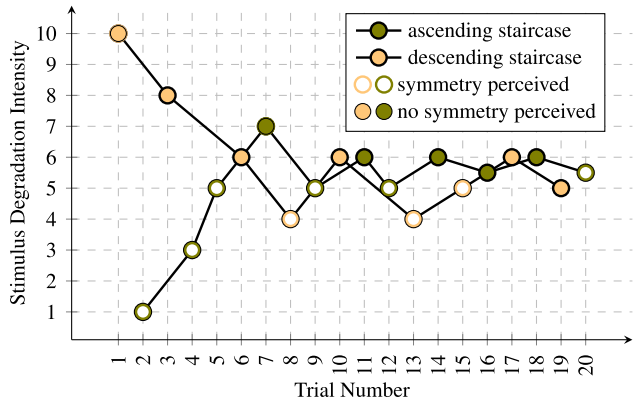

FIGURE 3. Two interleaved up-down staircases. Sample convergence of threshold is illustrated for two interleaved threshold determination processes.

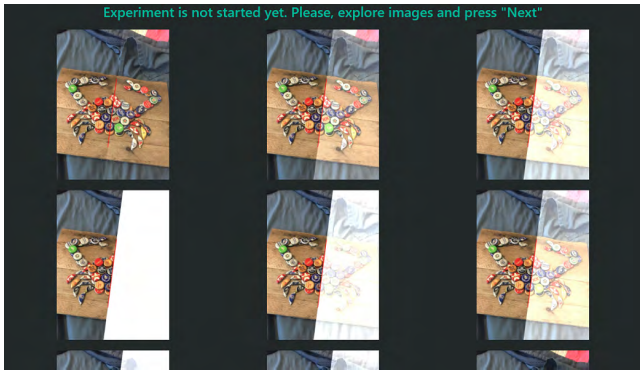

FIGURE 4. A screenshot from the web page describing sample stressed images. Stressed images are presented for building up the perceptual space in the human brain.

the human brain to develop a perceptual scale and measure for each visual stress. Fig. 4 illustrates a screenshot from the web-based system for sample images with LH stress type. After exploring all samples with various stress level from all visual stress types, the actual experiment starts. On the experiment page, a participant is requested to select one of two choices: ''symmetry'' or ''not symmetry'' for each presenting stressed image. The user interface also provides the tentative experiment progress. Fig. 5 shows the screenshot of the experiment page.

D. HUMAN EXPERIMENTS

1) EXPERIMENT 1: ABSOLUTE THRESHOLD FOR EACH IMAGE OF VISUAL STRESS TYPES

In this experiment, for all 55 images (5 images for each visual stress type), two interleaved processes are created. A process describes one up-down staircase with at least 20 trials for each. At each presentation, one visual stress type is selected randomly among eleven. Afterward, one image from the dataset of that stress type is randomly selected. Then, one staircase process is randomly selected out of two staircases. Based on the previous response of a participant on that

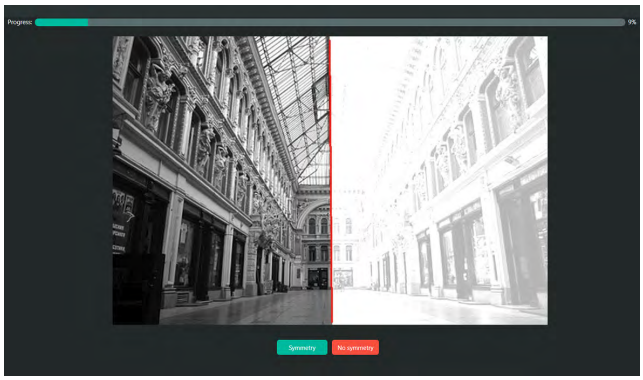

FIGURE 5. A screenshot of the experiment page. A stressed image is presented, and a participant's response is collected. The progress of experiment completing is also displayed.

process, the next image is generated by applying stress of newly updated intensity and presented to the participant. Then the participant gives his feedback to that presented stressed image and requests the next one to present. This procedure lasts until all processes terminate. 10 participants attended in this experiment. The absolute threshold is selected at stress intensity getting 50% population vote on the psychometric function of each image.

Fig. 6 provides the results of the psychophysical experiment by describing the absolute threshold distributions as a box plot for each image of visual stress types. For images of R, SA, and SC stress types, the threshold values have narrow distributions, and threshold medians are also close to each other. For the other stress types, the threshold distributions are various, because the nature of how the applied stress changes symmetry pattern depends on the content of the image as well. However, for the majority of images, the perception thresholds are still close: For each of BH, BW, DW, DH, LH, NH stress types, the medians of thresholds of 4 images out of all five images have close values. For each of NW and LW, the thresholds of 3 images out of all five images are close to each other.

2) EXPERIMENT 2: ABSOLUTE THRESHOLD FOR EACH VISUAL STRESS TYPE

The primary goal of this experiment is to detect the human perception threshold for each visual stress type. Unlike Experiment 1, which runs separate staircases for each image of visual stress type, in experiment 2, we create two interleaved staircases for each visual stress type. The maximum number of trials (presentations) for the progress is 50. For each visual stress type, at each presentation, stressed image is randomly selected and presented with stress intensity that is calculated based on the participant's response to the previously presented stressed image. In other words, all images of a particular visual stress type share the same staircase process. Over 40 participants attended this experiment in total, and for each visual stress type, thresholds of over 25 participants are collected. Fig. 7 illustrates a box plot that describes the distribution of threshold values for each visual stress type.

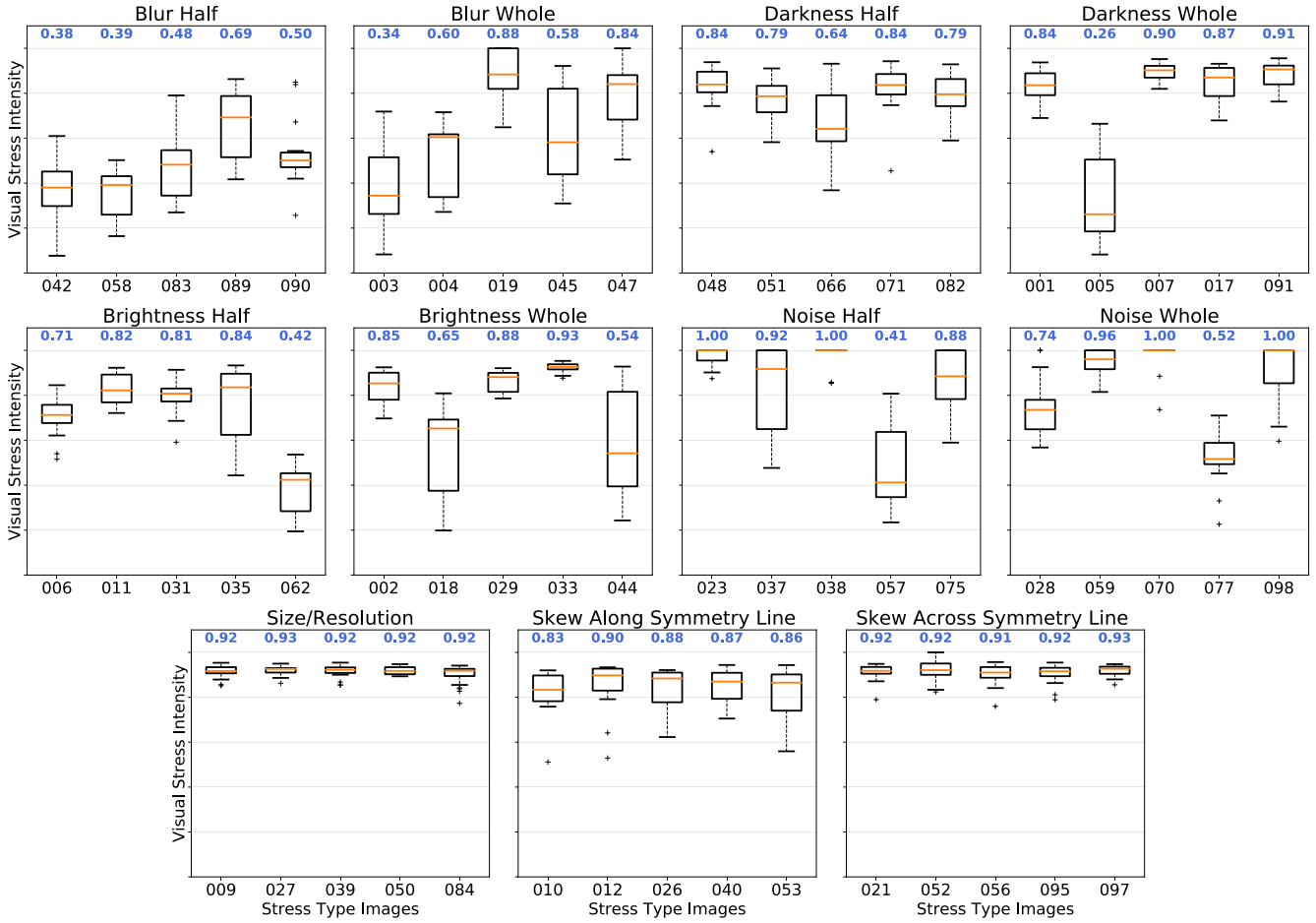

FIGURE 6. Threshold Distribution for each image of visual stress types.

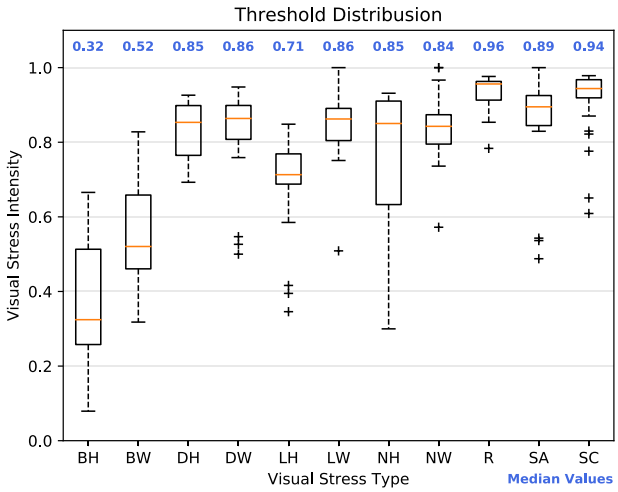

FIGURE 7. Distributions of participants' absolute thresholds for various visual stress types.

The absolute thresholds for BH, BW, and NH have broader distributions (high variance) than others. The average of the median thresholds in experiment 1 is consistent with those in experiment 2. We use the threshold values of experiment 2 for building our evaluation threshold. See figure 8 to observe sample stressed images that can be perceived as symmetry by humans.

IV. EVALUATION FRAMEWORK

Conventional evaluation of the reflection symmetry detection methods does not provide necessary insight into their behaviors on various visual stresses. However, the evaluation technique, which can demonstrate the limitations and advantageous aspects of detection methods, is beneficial and helpful in their further improvement. This kind of evaluation can also help to point out the applications where they can play best. In this section, we propose the evaluation technique that contains the properties mentioned above. The first proposing evaluation technique evaluates the performance of symmetry detection methods over increasing visual stress intensity. This technique shows how the evaluating method reacts to the visual stress types. The second evaluation technique that we propose unleashes the detection limits (the best possible performance) of the evaluating methods on particular visual stress type.

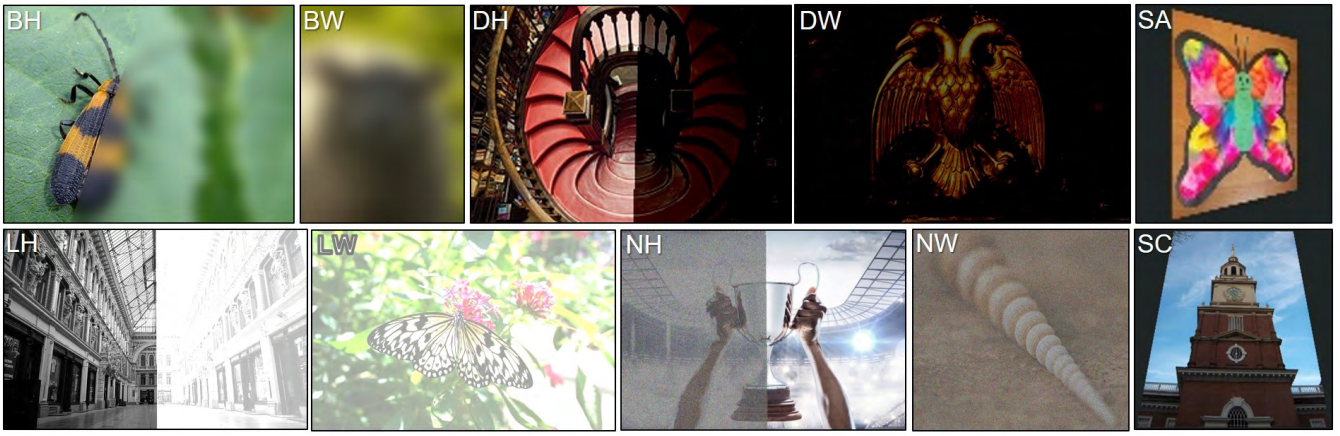

FIGURE 8. Stressed image samples with human perceivable reflection symmetry.

Before moving to the detailed descriptions of these techniques, let's introduce necessary notations and performance measures. Denote the symmetry decision rule *SDR* as a function of τ, and call τ a symmetry decision threshold. The symmetry decision threshold τ indicates the decision boundary between symmetry and non-symmetry ones of stressed symmetry images. In other words, given a reflection symmetry image, τ indicates the maximum intensity of visual stress in the image at which the stressed image still keeps its symmetry property. An image with stress intensity above τ has no symmetric pattern and is considered as non-symmetric. We can write the formulation of *SDR* function as follows:

$$SDR(I,\tau) = \begin{cases} 1, & \text{if } d_I <= \tau \\ 0, & \text{if } d_I > \tau \end{cases} \quad (1)$$

where I is the stressed image and d_I is the intensity of stress applied to the image I. Using the rule *SDR* one can separate stressed images of specific visual stress type into two categories: S - symmetry set and NS - non-symmetry set: $S = \{I|SDR(I,\tau) = 1\}$ and $SN = \overline{S} = \{I|SDR(I,\tau) = 0\}$.

Let's denote the set D of stressed images that are detected as symmetry by the symmetry detection method. Note that evaluation ignores all detections that are not labeled. Then, given set D, the formulation of performance parameters, the true positive, false positive, true negative and false negative, look follows:

$$TP = S \cap D$$
$$FP = NS \cap D$$
$$TN = S \cap \overline{D}$$
$$FN = SN \cap \overline{D}$$

A. EVALUATION TECHNIQUE 1

The first evaluation technique is about demonstrating the behavior of symmetry detection methods over increasing stress intensity. For this evaluation, the symmetry decision threshold is fixed at human symmetry perception threshold. In order to show the performance trend, performance score is calculated at each visual stress intensity. F1-score as a performance measure might include redundant calculations. Because, if we denote the L as a set of images that have the same intensity of a specific visual stress type, then L is a subset of either set S or set NS. If images of L belong to S, then the set D of images detected as symmetry is equal to true positives TP. Calculating precision Pr is redundant (always 1) and makes the F1-score represent only recall Rr (also called true positive rate TPR). Similarly, if images of set L belong to NS, then precision Pr is still redundant as there is no true positive TP detection, and the recall is also undefined because of empty S. So, in this case, true negative rate, $TNR = \frac{|TN|}{|TN|+|FP|}$ is used as a performance measure. So, in second evaluation, we use true detection rate TDR as performance measure:

$$TDR = \begin{cases} TPR, & \text{if } L \subset S \\ TNR, & \text{if } L \subset NS \end{cases} \quad (2)$$

B. EVALUATION TECHNIQUE 2

The second evaluation technique focuses on analyzing the performance of the computational symmetry detection method under various symmetry decision thresholds (*SDR*) of a specific visual stress type. It also determines the best possible performance and its corresponding decision threshold. In order to measure the performance of symmetry detection method on a specific stress type, f1-score is used:

$$F1 = \frac{2 * Pr * Rc}{Pr + Rc} \quad (3)$$

where, $Pr = \frac{|TP|}{|D|}$, $Rc = \frac{|TP|}{|S|}$, and $|.|$ denotes length of a set/class.

V. EVALUATION RESULTS

In this section, using the proposed evaluation techniques, we evaluate three state-of-the-art methods: Reflection Symmetry Detection via Appearance of Structure Descriptor [60], Wavelet-based Reflection Symmetry Detection via Textural and Color Histograms [61], and Detecting Symmetry and

Symmetric Constellations of Features [67]. These are top three well-performed methods in single 2D symmetry detection based on symmetry competition in ICCV 2017 workshop [26]. In order to detect symmetry patterns, Atadajanov and Lee [60] introduce appearance of structure features, which uses edges and contours in neighborhood. The method proposed by Elawady *et al.* [61] extracts edge/corner features using Log-Gabor filter, and describes them by their color and texture information in order to find reflected features. The method proposed by Loy and Eklundh [67] uses SIFT features for symmetric pattern detection.

For correct symmetry detection, we use the same rule provided in [28]. Two threshold values, t_1 and t_2, are used to determine correct detection. Successful detection happens, if the angle θ between detected symmetry axis s and provided ground truth g is smaller than first threshold t_1 and the distance δ to ground truth symmetry axis from the center of detected symmetry axis is smaller than second threshold t_2. In this evaluation $t_1 = 3\,\text{deg}$ and $t_2 = 0.025\,\min(height, width)$.

First, we evaluate the behavior of the computational symmetry detection methods by using the evaluation technique 1. Second, we determine the performance trends and the best possible performance values by using the evaluation technique 2.

A. BEHAVIOR EVALUATION OVER INCREASING SYMMETRY STRESS INTENSITY

Before moving to the analysis, let's define some terms (nouns and adjectives) that we use to describe the behavior of the methods in the context of proposed evaluation framework. Following are the necessary behavior properties which are vital to describe the performance and its behaviors.

- *Performance score* - a numerical value that indicates the performance of the detection method (e.g., true detection rate *TDR*).
- *Regularity* - a term describing common (expected or regular) behavior of the performance trend; non-increasing trend of performance measure is considered *regular*. Naturally, the expected trend of the performance measure is non-increasing as the intensity of stress increases. The opposite trend behavior is described by adjective, *irregular*.
- *Stability* - a term describing the frequency of the change in performance trend. A trend having fewer fluctuations (no fluctuation in an ideal case) is considered *stable*. So, the opposite trend performance behavior is *fluctuating* or *unstable*.

Our human annotated dataset provides the human perception threshold for various visual stresses. Based on these thresholds, images can be separated into two categories. ''positive'' (symmetry) and ''negative'' (non-symmetry). Fig. 9 illustrates the behavior of detection methods defined by their true detection rate (TDR), which is equal to either true positive rate, TPR, (Sensitivity) or true negative rate, TNR, (Specificity). The trend of TDR along visual stress intensity is presented. Unlike human perception, which usually has monotonic behavior on these visual stress intensities, most of the computational methods get the non-monotonic and fluctuating behavior. Behavior-wise, the method proposed by Elawady *et al.* [61] seems more stable than the others; it has a small variance of TDR along stress intensity. However, the method proposed by Loy and Eklundh [67] achieves overall the highest trend despite getting TDR level fluctuated. The method provided by Atadjanov and Lee [60] has very diverse TDR values throughout the stress intensity space. Below, we analyze the results for each visual stress type separately.

1) BLURRING

Based on the results of human perception experiment, blurring creates a strong perceptual visual stress to reflection symmetry. Performance of the method provided by Atadjanov and Lee [60] drops almost to the half its initial performance with only small amounts of blurring applied. Detection method provided by them uses edge-based and contour-based features that describe the appearance of the image structure. Blurring the image fades the edges out and create new edges. Therefore, when the blurring applied to one half of the symmetry pattern, the strength of structure on that half decreases dramatically and achieves not similar descriptions. Contrarily, the features used by Loy and Eklundh [67] are SIFT. In consequence, this method gets the highest TDR scores. For images with the whole content blurred, the method proposed in [61] achieves the most stable TDR score in symmetry detection. In this evaluation, the methods proposed in [61] and [67] achieve stable and relatively high TPR till reaching the human symmetry perception threshold. For negative detection part, methods proposed in [60] achieves the highest and stable TDR.

2) BRIGHTNESS

Changing the brightness of the image decreases the strength of both structure and appearance. However, changing brightness does not create new edges or change the location of features. Hence, the method given in [60] achieves much stable TDR values, unlike the blurring stress. However, the method still performs worse than the method introduced in [67] in the positive (symmetry) detection job. The method given in [61] achieves the worst TDR on BH stress type. In the non-symmetry detection job, the methods proposed in [60] and [67] perform competitively equal and get the highest TDR. For DW and BW stress type, the method provided in [61] achieves the best performance near the human perception threshold values. It makes the method provided by Elawady *et al.* [61] the most robust against brightness changing stress on the whole image (BW and DW). For BH stress type, the methods proposed by Loy and Eklundh [67], and Atadjanov and Lee [60] yield competitive performances.

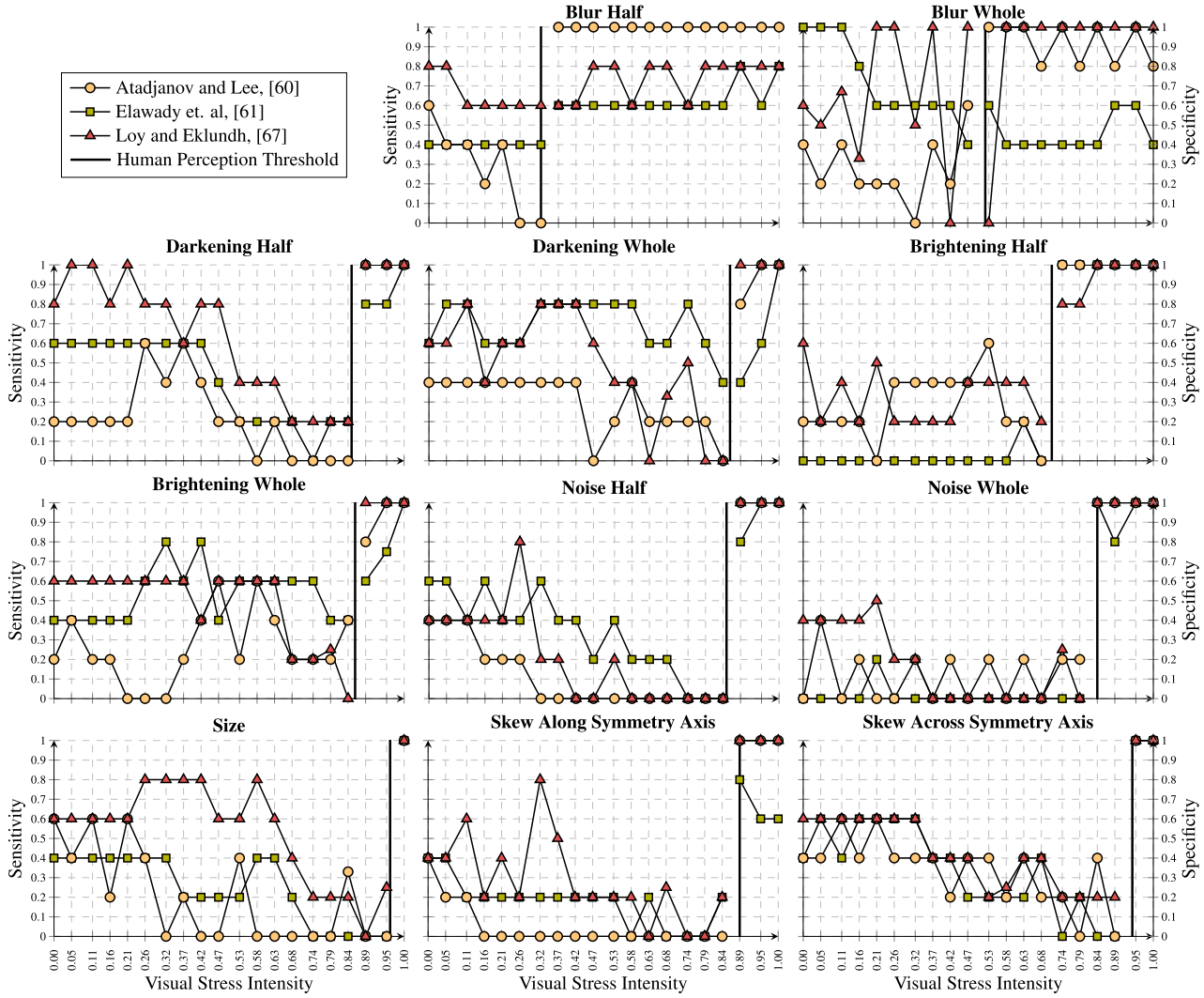

FIGURE 9. Behavior evaluation of computational reflection symmetry methods along visual stress intensity. Sensitivity is calculated positive detection job (before threshold), and specificity is calculated for negative detection job after the threshold.

3) NOISE

Stressing the symmetry image by adding white noise is one of the most challenging visual stress types for all methods. Performance of methods proposed in [60] and [67] drop to zero before reaching half strength of noise which is applied to half of the symmetry pattern (NH). However, the method introduced in [61] achieves a non-zero performance in much larger intensity range before stress reaches the threshold value. It also has more stable behavior with having its performance decreasing gradually. For NW visual stress type, the method proposed in [67] achieves the highest performance, especially at low intensities. Unlike NH stress type, the method proposed by Elawady *et al.* [61] achieves the worst performance against NW stress type. For NW, we cannot judge the behavior of the method introduced in [61] as it cannot detect symmetry in original (unstressed) images.

4) SIZE

The performance of all three methods drop to zero before reaching the threshold. Generally, the method proposed by Loy and Eklundh [67] has a high trend of performance values. Performance trend of the method has only two fluctuations which make the method the second best in being regular and stable. The performance trend of the method proposed in [60] has the most unstable and unpredictable form. The method yielded the worse performance on average for the stress type. The method of Elawady *et al.* [61] achieves a more regular and stable trend of all three trends.

5) SKEWNESS

Human symmetry perception is robust to viewpoint change. Therefore, the psychophysical experiment achieved a high skew threshold. For all methods, the performance is dropped to zero before the stress intensity reaches the threshold in

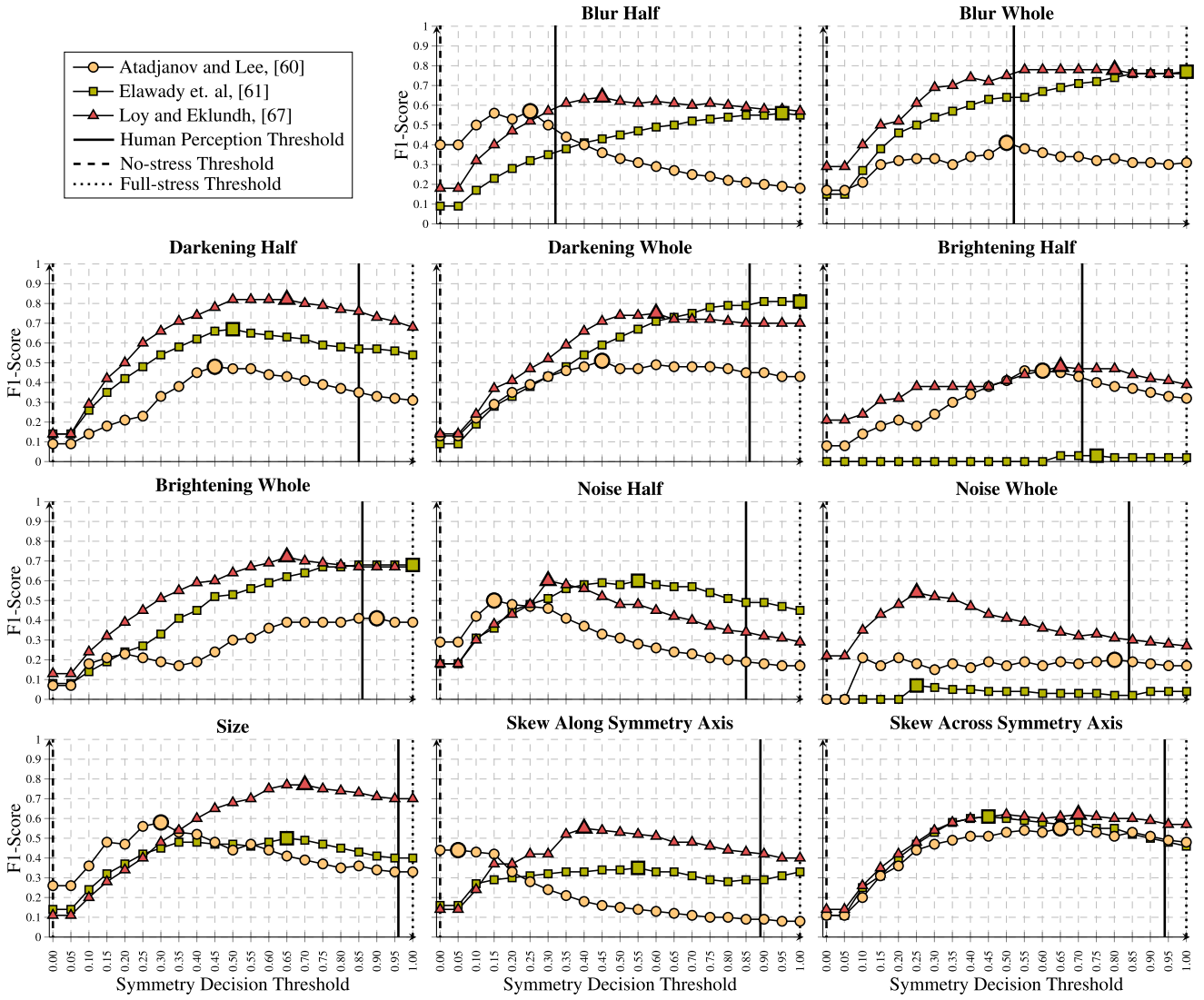

FIGURE 10. F1-score of computational reflection symmetry detection methods for each visual stress type with various symmetry decision threshold values.

SC stress type. The method provided in [67] has the most irregular and fluctuating trend but the highest performance score. The method proposed by Atadjanov and Lee [60] has a more regular trend but the lowest performance score. The method introduced in [61] also has a regular trend.

B. PERFORMANCE EVALUATION ON VARIOUS SYMMETRY DECISION BOUNDARY

We evaluated the performance of the computational methods for each visual stress type by varying the symmetry decision threshold over stress intensity. Fig. 10 illustrates the performance trend and peak performance for each of three methods over the symmetry decision threshold axis. Based on the trend, the method proposed by Loy and Eklundh [67] achieves high performance over a larger portion of the abscissa axis. It also has higher peak value on all visual stress types except DH. However, for BH, NH, R and SA visual stress types method provided by [60] achieves higher performance on the lower values of the symmetry decision threshold. For only perfect (more perfect and less stressed) symmetry detection application, the method proposed in [60] achieves the highest performance. Table 1 provides exact performance scores with the symmetry decision threshold at the no-stress threshold, full-stress threshold and human perception threshold. The method provided in [67] achieves the best overall performance with the symmetry decision threshold at the full-stress threshold and the human perception threshold. However, the method provided by Atadjanov and Lee [60] performs the best on the no-stress threshold. The method proposed by Elawady *et al.* [61] outperforms other two methods in DW and NH stress types at high values of symmetry decision threshold. For stress type SC, all three methods get relatively close performance scores over all symmetry decision thresholds. Considering the whole symmetry decision space and all visual stress types, the method provided in [67] is the best, while the method provided in [61] is the second

TABLE 1. F1-score of computational reflection symmetry detection methods for three symmetry decision thresholds.

Visual Stress Types	No-stress Threshold			Full-stress Threshold			Human Perception Threshold		
	Atadjanov and Lee [61]	Loy and Eklundh [68]	Elawady et. al [62]	Atadjanov and Lee [61]	Loy and Eklundh [68]	Elawady et. al [62]	Atadjanov and Lee [61]	Loy and Eklundh [68]	Elawady et. al [62]
Blur Half	**0.40**	**0.18**	0.09	0.18	**0.57**	**0.55**	**0.44**	**0.61**	0.38
Blur Whole	**0.17**	**0.29**	0.15	0.31	**0.76**	**0.77**	0.41	**0.75**	**0.64**
Darkening Half	0.09	**0.14**	**0.143**	0.31	**0.68**	**0.54**	0.35	**0.76**	**0.57**
Darkening Whole	**0.13**	**0.14**	0.09	0.43	**0.70**	**0.81**	0.45	**0.70**	**0.79**
Brightening Half	**0.08**	**0.21**	0.00	**0.32**	**0.39**	0.02	**0.43**	**0.47**	0.03
Brightening Whole	0.07	**0.13**	**0.08**	0.39	**0.67**	**0.68**	0.41	**0.67**	**0.68**
Noise Half	**0.29**	**0.182**	0.173	0.17	**0.29**	**0.45**	0.19	**0.34**	**0.49**
Noise Whole	0.00	**0.22**	0.00	**0.17**	**0.27**	0.04	**0.20**	**0.31**	0.02
Size	**0.26**	0.11	**0.14**	0.33	**0.70**	**0.40**	0.33	**0.70**	**0.40**
Skew Along Symmetry Axis	**0.44**	0.14	**0.16**	0.08	**0.40**	**0.33**	0.09	**0.43**	**0.29**
Skew Across Symmetry Axis	0.11	**0.14**	0.11	**0.48**	**0.57**	0.46	**0.51**	**0.59**	0.50
All Stimuli	**0.159**	**0.157**	0.12	0.29	**0.55**	**0.49**	0.35	**0.59**	**0.48**

best in performance measure among three symmetry detection methods.

VI. CONCLUSION

In this work, we proposed a novel evaluation framework for computational symmetry detection methods based on human symmetry perception. The proposed framework evaluates the robustness and behavior of computational reflection symmetry detection methods on various visual stresses. Initially, we determined human symmetry perception limits on 11 visual stress types. For that, we conducted a psychophysical experiment. We, psychophysically, showed that the thresholds for each visual stress types are consistent with individual thresholds of images for those visual stress types. We introduced modifications to the up-down staircase method and developed a web-based system to conduct the psychophysical experiment. Based on human perception limits, we built a human annotated dataset for all 11 stress types with various stress intensities and introduced necessary performance measures for the proposed evaluation framework. We evaluated three state-of-the-art computational reflection symmetry detection methods using the proposed framework. The proposed evaluation framework showed how the evaluating methods are robust to various visual stress and behavior of evaluating methods as a function of stress intensity. In our view, the proposed evaluation framework provides more increased insight into the weak and strong aspects of the evaluating methods than the traditional evaluations could do.

REFERENCES

[1] M. Giurfa, A. Dafni, and P. R. Neal, "Floral symmetry and its role in plant-pollinator systems," *Int. J. Plant Sci.*, vol. 160, no. S6, pp. S41–S50, 1999.

[2] Y. Liu, H. Hel-Or, C. S. Kaplan, and L. Van Gool, "Computational symmetry in computer vision and computer graphics," *Found. Trends Comput. Graph. Vis.*, vol. 5, nos. 1–2, pp. 1–195, 2009.

[3] C. W. Tyler, Ed., *Human Symmetry Perception and Its Computational Analysis*. Mahwah, NJ, USA: Lawrence Erlbaum Associates, 2002.

[4] A. P. Møller, "Female swallow preference for symmetrical male sexual ornaments," *Nature*, vol. 357, no. 6375, pp. 238–240, 1992.

[5] J. P. Swaddle and I. C. Cuthill, "Preference for symmetric males by female zebra finches," *Nature*, vol. 367, no. 6459, pp. 165–166, 1994.

[6] M. Giurfa, B. Eichmann, and R. Menzel, "Symmetry perception in an insect," *Nature*, vol. 382, no. 6590, pp. 458–461, 1996.

[7] A. P. Møller, "Bumblebee preference for symmetrical flowers," *Proc. Nat. Acad. Sci. USA*, vol. 92, no. 6, pp. 2288–2292, 1995.

[8] G. A. Horridge, "The honeybee (*apis mellifera*) detects bilateral symmetry and discriminates its axis," *J. Insect Physiol.*, vol. 42, no. 8, pp. 755–764, 1996.

[9] M. Enquist and A. Arak, "Symmetry, beauty and evolution," *Nature*, vol. 372, no. 6502, pp. 169–172, 1994.

[10] R. A. Johnstone, "Female preference for symmetrical males as a by-product of selection for mate recognition," *Nature*, vol. 372, no. 6502, pp. 172–175, 1994.

[11] G. Rhodes, F. Proffitt, J. M. Grady, and A. Sumich, "Facial symmetry and the perception of beauty," *Psychon. Bull. Rev.*, vol. 5, no. 4, pp. 659–669, 1998.

[12] T. Vetter and T. Poggio, "Symmetric 3D objects are an easy case for 2D object recognition," *Spatial Vis.*, vol. 8, no. 4, pp. 443–453, 1994.

[13] J. J. DiCarlo, D. Zoccolan, and N. C. Rust, "How does the brain solve visual object recognition?" *Neuron*, vol. 73, no. 3, pp. 415–434, 2012.

[14] R. L. DeValois and K. K. DeValois, *Spatial Vision*, vol. 14. London, U.K.: Oxford Univ. Press, 1990.

[15] N. V. S. Graham, *Visual Pattern Analyzers*. London, U.K.: Oxford Univ. Press, 1989.

[16] D. H. Hubel and T. N. Wiesel, "Receptive fields and functional architecture of monkey striate cortex," *J. Physiol.*, vol. 195, no. 1, pp. 215–243, 1968.

[17] H. R. Wilson, "Pattern discrimination, visual filters, and spatial sampling irregularity," in *Computational Models of Visual Processing*. Cambridge, MA, USA: MIT Press, 1991, pp. 153–168.

[18] W. H. Merigan, "Basic visual capacities and shape discrimination after lesions of extrastriate area V4 in macaques," *Vis. Neurosci.*, vol. 13, no. 1, pp. 51–60, 1996.

[19] A. Pasupathy and C. E. Connor, "Population coding of shape in area V4," *Nature Neurosci.*, vol. 5, no. 12, pp. 1332–1338, 2002.

[20] D. C. Van Essen, "Functional organization of primate visual cortex," *Cerebral Cortex*, vol. 3, pp. 259–329, 1985.

[21] M. P. Young, "Objective analysis of the topological organization of the primate cortical visual system," *Nature*, vol. 358, no. 6382, pp. 152–155, 1992.

[22] Y. Sasaki, W. Vanduffel, T. Knutsen, C. Tyler, and R. Tootell, "Symmetry activates extrastriate visual cortex in human and nonhuman primates," *Proc. Nat. Acad. Sci. USA*, vol. 102, no. 8, pp. 3159–3163, 2005.

[23] C. W. Tyler, H. A. Baseler, L. L. Kontsevich, L. T. Likova, A. R. Wade, and B. A. Wandell, "Predominantly extra-retinotopic cortical response to pattern symmetry," *NeuroImage*, vol. 24, no. 2, pp. 306–314, 2005.

[24] T. Serre and T. Poggio, "A neuromorphic approach to computer vision," *Commun. ACM*, vol. 53, no. 10, pp. 54–61, 2010.
[25] S. Lee and Y. Liu, "Curved glide-reflection symmetry detection," *IEEE Trans. Pattern Anal. Mach. Intell.*, vol. 34, no. 2, pp. 266–278, Feb. 2012.
[26] C. Funk *et al.*, "2017 ICCV challenge: Detecting symmetry in the wild," in *Proc. ICCV Workshop*, Oct. 2017, pp. 1692–1701.
[27] I. Rauschert, J. Liu, K. Brockelhurst, S. Kashyap, and Y. Liu, "Symmetry detection competition: A summary of how the competition is carried out," in *Proc. IEEE Conf. Comput. Vis. Pattern Recognit., Workshop, Symmetry Detection Real World Images*, Jun. 2011, pp. 1–66.
[28] J. Liu *et al.*, "Symmetry detection from realworld images competition 2013: Summary and results," in *Proc. IEEE Conf. Comput. Vis. Pattern Recognit. Workshops (CVPRW)*, Jun. 2013, pp. 200–205.
[29] R. Nagar and S. Raman, "SymmMap: Estimation of the 2-D reflection symmetry map and its applications," in *Proc. ICCV Workshop*, Oct. 2017, pp. 1715–1724.
[30] R. Nagar and S. Raman. (Jun. 2017). "Approximate reflection symmetry in a point set: Theory and algorithm with an application." [Online]. Available: http://arxiv.org/abs/1706.08801
[31] G. Allen, "The origin of the sense of symmetry," *Mind*, vol. 4, no. 15, pp. 301–316, 1879.
[32] M. Bertamini and A. D. J. Makin, "Brain activity in response to visual symmetry," *Symmetry*, vol. 6, no. 4, pp. 975–996, 2014.
[33] H. R. Wilson and F. Wilkinson, "Symmetry perception: A novel approach for biological shapes," *Vis. Res.*, vol. 42, no. 5, pp. 589–597, 2002.
[34] C. W. Tyler, "Human symmetry perception," in *Human Symmetry Perception and Its Computational Analysis*. Utrecht, The Netherlands: VSP (VNU Science Press), 1996, pp. 3–22.
[35] V. G. Bruce and M. J. Morgan, "Violations of symmetry and repetition in visual patterns," *Perception*, vol. 4, no. 3, pp. 239–249, 1975.
[36] H. B. Barlow and B. C. Reeves, "The versatility and absolute efficiency of detecting mirror symmetry in random dot displays," *Vis. Res.*, vol. 19, no. 7, pp. 783–793, 1979.
[37] B. Jenkins, "Redundancy in the perception of bilateral symmetry in dot textures," *Perception Psychophys.*, vol. 32, no. 2, pp. 171–177, 1982.
[38] C. W. Tyler, L. Hardage, and R. T. Miller, "Multiple mechanisms for the detection of mirror symmetry," *Spatial Vis.*, vol. 9, no. 1, pp. 79–100, 1995.
[39] S. C. Dakin and A. M. Herbert, "The spatial region of integration for visual symmetry detection," *Proc. Roy. Soc. London B, Biol. Sci.*, vol. 265, no. 1397, pp. 659–664, 1998.
[40] C. W. Tyler, "Human symmetry detection exhibits reverse eccentricity scaling," *Vis. Neurosci.*, vol. 16, no. 5, pp. 919–922, 1999.
[41] R. Gurnsey, A. M. Herbert, and J. Kenemy, "Bilateral symmetry embedded in noise is detected accurately only at fixation," *Vis. Res.*, vol. 38, no. 23, pp. 3795–3803, 1998.
[42] B. T. Barrett, D. Whitaker, P. V. McGraw, and A. M. Herbert, "Discriminating mirror symmetry in foveal and extra-foveal vision," *Vis. Res.*, vol. 39, no. 22, pp. 3737–3744, 1999.
[43] U. Koeppl and M. Morgan, "Local orientation versus local position as determinants of perceived symmetry," *Perception*, vol. 22, p. 111, 1993.
[44] J. Wagemans, L. Van Gool, V. Swinnen, and J. Van Horebeek, "Higher-order structure in regularity detection," *Vis. Res.*, vol. 33, no. 8, pp. 1067–1088, 1993.
[45] S. C. Dakin and R. F. Hess, "The spatial mechanisms mediating symmetry perception," *Vis. Res.*, vol. 37, no. 20, pp. 2915–2930, 1997.
[46] J. A. Saunders and D. C. Knill, "Perception of 3D surface orientation from skew symmetry," *Vis. Res.*, vol. 41, no. 24, pp. 3163–3183, 2001. [Online]. Available: http://www.sciencedirect.com/science/article/pii/S0042698901001870
[47] J. Wagemans, "Skewed symmetry: A nonaccidental property used to perceive visual forms," *J. Experim. Psychol., Hum. Perception Perform.*, vol. 19, no. 2, pp. 364–380, 1993.
[48] L. Zhang, "Symmetry perception in human vision," in *Psychology (Companions to Ancient Thought: 2)*, S. Everson, Ed. New York, NY, USA: Cambridge Univ. Press, 1991.
[49] P. Wenderoth, "The effects of the contrast polarity of dot-pair partners on the detection of bilateral symmetry," *Perception*, vol. 25, no. 7, pp. 757–771, 1996.
[50] P. Carlin, "On symmetry in visual perception," Ph.D dissertation, Dept. Psychol., Univ. Stirling, Stirling, Scotland, 1996.
[51] P. A. van der Helm and E. L. J. Leeuwenberg, "Accessibility: A criterion for regularity and hierarchy in visual pattern codes," *J. Math. Psychol.*, vol. 35, no. 2, pp. 151–213, May 1991.
[52] P. A. Van Der Helm and E. L. Leeuwenberg, "Goodness of visual regularities: A nontransformational approach," *Psychol. Rev.*, vol. 103, no. 3, pp. 429–456, 1996.
[53] J. Wagemans, "Detection of visual symmetries," in *Human Symmetry Perception and Its Computational Analysis*. New York, NY, USA: Psychology Press, 2003, pp. 31–54.
[54] J. Wagemans, "Toward a better approach to goodness: Comments on Van der Helm and Leeuwenberg (1996)," *Psychol. Rev.*, vol. 106, no. 3, pp. 610–621, 1999.
[55] P. A. van der Helm and E. L. J. Leeuwenberg, "A better approach to goodness: Reply to Wagemans (1999)," *Psychol. Rev.*, vol. 106, no. 3, pp. 622–630, 1999.
[56] P. A. van der Helm and E. L. J. Leeuwenberg, "Holographic goodness is not that bad: Reply to olivers, chater, and watson (2004)," *Psychol. Rev.*, vol. 111, no. 1, pp. 261–273, 2004.
[57] M. Nucci and J. Wagemans, "Goodness of regularity in dot patterns: Global symmetry, local symmetry, and their interactions," *Perception*, vol. 36, no. 9, pp. 1305–1319, 2007.
[58] S. C. Dakin and R. J. Watt, "Detection of bilateral symmetry using spatial filters," *Spatial Vis.*, vol. 8, no. 4, pp. 393–413, Jan. 1994.
[59] I. Atadjanov and S. Lee, "Bilateral symmetry detection based on scale invariant structure feature," in *Proc. IEEE Int. Conf. Image Process. (ICIP)*, Sep. 2015, pp. 3447–3451. [Online]. Available: http://ieeexplore.ieee.org/document/7351444/
[60] I. R. Atadjanov and S. Lee, "Reflection symmetry detection via appearance of structure descriptor," in *Computer Vision—ECCV* (Lecture Notes in Computer Science). 2016, pp. 3–18.
[61] M. Elawady, C. Ducottet, O. Alata, and P. Colantoni, "Wavelet-based reflection symmetry detection via textural and color histograms," in *Proc. ICCV Workshop*, 2017, pp. 1725–1733.
[62] R. Nagar and S. Raman, "Reflection symmetry axes detection using multiple model fitting," *IEEE Signal Process. Lett.*, vol. 24, no. 10, pp. 1438–1442, Oct. 2017. [Online]. Available: http://ieeexplore.ieee.org/document/8000660/
[63] A. Gnutti, F. Guerrini, and R. Leonardi, "On reflection symmetry in natural images," in *Proc. 15th Int. Workshop Content-Based Multimedia Indexing (CBMI)*, New York, NY, USA: ACM Press, 2017, pp. 1–7. [Online]. Available: http://dl.acm.org/citation.cfm?doid=3095713.3095743
[64] A. Gnutti, F. Guerrini, and R. Leonardi, "A normalized mirrored correlation measure for data symmetry detection," in *Proc. 25th Eur. Signal Process. Conf. (EUSIPCO)*, Aug./Sep. 2017, pp. 813–817.
[65] M. Elawady, O. Alata, C. Ducottet, C. Barat, and P. Colantoni, "Multiple reflection symmetry detection via linear-directional kernel density estimation," in *Computer Analysis of Images and Patterns* (Lecture Notes in Computer Science), vol. 10424. Cham, Switzerland: Springer, 2017, pp. 344–355. [Online]. Available: https://arxiv.org/abs/1704.06392
[66] M. Cicconet, D. G. C. Hildebrand, and H. Elliott, "Finding mirror symmetry via registration and optimal symmetric pairwise assignment of curves," in *Proc. ICCV Workshop*, Oct. 2017, pp. 1749–1758.
[67] G. Loy and J.-O. Eklundh, "Detecting symmetry and symmetric constellations of features," in *Proc. 9th Eur. Conf. Comput. Vis.*, vol. 3952. Berlin, Germany: Springer-Verlag, 2006, pp. 508–521.
[68] R. Geirhos, D. H. J. Janssen, H. H. Schütt, J. Rauber, M. Bethge, and F. A. Wichmann. (2017). "Comparing deep neural networks against humans: Object recognition when the signal gets weaker." [Online]. Available: https://arxiv.org/abs/1706.06969
[69] S. Dodge and L. Karam, "A study and comparison of human and deep learning recognition performance under visual distortions," in *Proc. 26th Int. Conf. Comput. Commun. Netw. (ICCCN)*, Jul. 2017, pp. 1–7.
[70] P. A. van der Helm, "Weber-fechner behavior in symmetry perception?" *Attention, Perception, Psychophys.*, vol. 72, no. 7, pp. 1854–1864, 2010.
[71] T. N. Cornsweet, "The staircase-method in psychophysics," *Amer. J. Psychol.*, vol. 75, no. 3, pp. 485–491, Sep. 1962.
[72] G. A. Gescheider, *Psychophysics: The Fundamentals*. Mahwah, NJ, USA: Lawrence Erlbaum Associates, 1997. [Online]. Available: https://www.routledge.com/Psychophysics-The-Fundamentals-3rd-Edition/Gescheider/p/book/9780805822816
[73] H. Levitt, "Transformed up-down methods in psychoacoustics," *J. Acoust. Soc. Amer.*, vol. 49, no. 2B, pp. 467–477, 1971.

IBRAGIM R. ATADJANOV received the B.S. degree in applied mathematics and computer science from Urgench State University, Urgench, Uzbekistan, in 2008, and the M.S. degree in information security from the Tashkent University of Information Technologies, Tashkent, Uzbekistan, in 2011. He is currently pursuing the Ph.D. degree in computer science and engineering with Kyung Hee University, South Korea.

His research interests include feature detection and description, pattern recognition, symmetry-based computer vision, multilayer compressive light field displays, and deep learning.

SEUNGKYU LEE received the B.S. and M.S. degrees in electrical engineering from the Korea Advanced Institute of Science and Technology, Daejeon, South Korea, in 1997 and 1999, respectively, and the Ph.D. degree in computer science and engineering from The Pennsylvania State University in 2009.

He has been a Research Engineer with the Technical Research Institute, Korea Broadcasting System, Seoul, South Korea, where he has been involved in the research on high-definition image processing, MPEG4 advanced video coding, and the standardization of terrestrial-digital mobile broadcasting. He has also been a Principal Research Scientist with the Advanced Media Laboratory, Samsung Advanced Institute of Technology, Yongin, South Korea. He is currently an Associate Professor with Kyung Hee University, Seoul. His research interests include time-of-flight depth camera, color/depth image processing, symmetry-based computer vision, and 3-D modeling and reconstruction.